

Continuous measurement of soil CO₂ efflux in a larch forest by automated chamber and
concentration gradient techniques

Naishen Liang¹, T. Hirano², Z.-M. Zheng³, J. Tang⁴, and Y. Fujinuma^{1, 5}

¹Center for Global Environmental Research, National Institute for Environmental
Studies, Tsukuba, Ibaraki 305-8506, Japan

²Graduate School of Agriculture, Hokkaido University, Sapporo 060-0809, Japan

³East China Normal University, Shanghai 200062, China

⁴The Ecosystems Center, Marine Biological Laboratory, Woods Hole, MA 02543, USA

⁵Tottori University of Environmental Studies, Tottori 689-1111, Japan

Correspondence to: Naishen Liang (liang@nies.go.jp)

Abstract

We used two alternative systems for continuous measurement of ecosystem parameters associated with soil CO₂ efflux in a 45-year-old larch forest in northern Japan: (1) a 16-channel automated soil chamber system with eight chambers for CO₂ efflux and eight chambers for the heterotrophic respiration during snow-free periods, and (2) a soil gradient system for monitoring soil CO₂ concentration profiles year-round, including when the ground was snow-covered. While the automated chamber system has the advantages of being able to simultaneously partition soil CO₂ efflux into autotrophic (root) and heterotrophic components and evaluate their temporal and spatial variations, the gradient system can provide the vertical information of CO₂ production and transport at different soil depths. The gradient approach yielded slightly higher CO₂ effluxes than the automated chamber technique did during the warm season, but yielded slightly lower CO₂ effluxes during the cold season. The annual soil CO₂ efflux measured by the automated chamber system was 959 g C m⁻² (of which 57% was contributed by heterotrophic respiration) and 1040 g C m⁻² by the gradient system. A bias from the gradient measurement corresponds to about 8% of the annual soil CO₂ efflux; however the high agreement between measurements ($R^2 = 0.812$) suggests that the two systems can be used as complement of one another for inter-gap-filling of the

1 missing measurements. Both the chamber and the gradient system observed relatively
2 high Q_{10} values (between 3.1 and 4.5) and low sensitivities of the soil CO₂ efflux on
3 moisture, indicating that temperature was the most importance environmental factor
4 driving the soil CO₂ efflux in this forest. The gradient system measured the soil CO₂
5 effluxes ranging from 0.40 to 0.70 $\mu\text{mol m}^{-2} \text{s}^{-1}$ during the snow-covered season, and the
6 total CO₂ efflux from the snowpack was estimated to be about 73 g C m⁻². The chamber
7 system detected a large seasonality of soil CO₂ efflux Q_{10} and discovered that the root
8 respiration Q_{10} was dominantly responsible for the seasonal pattern of the soil CO₂
9 efflux Q_{10} . Furthermore, the fast-response chamber technique determined temporarily
10 higher effluxes following rain events that were responsible for about 2% of the annual
11 soil CO₂ efflux.

1 **1 Introduction**

2 The world's soils contain about 1550 Pg of organic carbon, which is more than twice the
3 amount in the atmosphere (IPCC, 2007). Forests worldwide contain about 45% of the
4 global carbon stock, a large part of which is in the forest soils. Recently,
5 Bond-Lamberty and Thomson (2010) estimated that the global soil CO₂ efflux, widely
6 referred to as soil respiration (R_s), was about 98 Pg C y⁻¹ in 2008 based on a five-decade
7 record of chamber measurements, which is more than 13 times the rate of fossil fuel
8 combustion (IPCC, 2007), indicating that 20-40% of the atmosphere's CO₂ circulates
9 through soils each year. Overall, R_s is the largest component of ecosystem respiration
10 and the second largest flux in the global carbon cycle after gross primary production
11 (GPP). It is therefore a key process that is fundamental to our understanding of the
12 terrestrial carbon cycle (Davidson and Janssens, 2006). A relatively small change in the
13 carbon flow into or out of soils can potentially strongly influence global cycles of
14 carbon, nitrogen, and water. For example, it has been reported that the global R_s
15 increased by 0.1 Pg C y⁻¹ between 1989 and 2008 (Bond-Lamberty and Thomson, 2010),
16 and the positive feedback from this enhancement of R_s by global warming would raise
17 the CO₂ concentration in the atmosphere by 20-224 ppm by 2100, and that resulting
18 higher CO₂ levels would lead to an additional temperature increase ranging between 0.1

1 and 1.5 °C (Friedlingstein et al., 2006; IPCC, 2007).

2 In forest ecosystems, micrometeorological studies (i.e., eddy covariance) have
3 shown that, on average, ~80% of GPP is respired back to the atmosphere (Law et al.,
4 2002), and R_s has been estimated to account for 60-90% of the total ecosystem
5 respiration, with marked temporal as well as spatial variations (Law et al.,
6 1999; Janssens et al., 2000; Liang et al., 2004). Therefore, R_s has recently received much
7 attention from researchers and its accurate measurement is critical for developing a
8 reliable model of carbon exchange in forest ecosystems (Jassal et al., 2007; Zhou et al.,
9 2009).

10 More than half of all terrestrial ecosystems in the Northern Hemisphere experience
11 substantial snow cover during the winter (Sommerfeld et al., 1993). However, little is
12 known about winter soil CO₂ efflux values, particularly those under the snowpack.
13 Because of difficulties of measurement and access, most annual estimates of soil CO₂
14 efflux have ignored the soil CO₂ winter efflux or have assumed that it is zero
15 (Fahnestock et al., 1999), or the wintertime efflux has been evaluated with simple
16 temperature-driven models (Liang et al., 2004).

17 Because R_s is highly variable spatially and the soil medium is not easily accessible,
18 R_s cannot be measured by large-scale remote sensing. FLUXNET has become an

1 effective network for observing carbon sequestration or loss by global terrestrial
2 ecosystems by the eddy covariance technique (Luyssaert et al., 2008). Unfortunately,
3 the use of the eddy covariance technique for measuring soil CO₂ efflux, especially
4 below forest canopies, is often hampered by relatively low wind speeds (Drewitt et al.,
5 2002) as well as by an abundance of understory vegetation (Lee, 1998; Janssens et al.,
6 2001). Therefore, to validate nocturnal, subcanopy, and bad-weather (e.g., rainy period)
7 eddy covariance measurements as well as the partition of the net ecosystem production
8 (NEP), the flux research community must use automated chamber systems, which can
9 make continuous (i.e., half-hourly or hourly) measurements of R_s (Gaumont-Guay et al.,
10 2009; Jassal et al., 2007). Moreover, the automated continuous measurements of R_s (see
11 (Goulden and Crill, 1997; Savage and Davidson, 2003; Liang et al., 2004)) provide
12 insights about ecosystem processes, which were not possible to explore before (Vargas
13 et al., 2010).

14 R_s is related to the carbon recently assimilated by plants (i.e. through the
15 respiration of roots, mycorrhizas and rhizosphere microorganisms) and the carbon
16 respired during the decomposition of dead plant litter, microbial debris and destabilized
17 soil organic matter (Hanson et al., 2000; Ryan and Law, 2005). The variation of CO₂
18 production in the soil profile changes soil CO₂ concentration gradients, which in

1 conjunction with changes in soil CO₂ diffusivity regulate R_s (Šimůnek and Suarez,
2 1993; Vargas et al., 2010). Based on Fick's Law of diffusion, R_s can be practicably
3 calculated from CO₂ concentrations at two or more depths of soil. This soil CO₂
4 gradient technique is generally conducted by extracting soil air with gas-tight syringes
5 from tubes inserted into different depths of soil, and measuring the CO₂ concentrations
6 of the extracted air subsequently in the laboratory with a gas chromatograph (Takle et
7 al., 2004) or infrared gas analyzer (IRGA) (Hubbard et al., 2005), or in the field with a
8 portable IRGA (Drewitt et al., 2005; Davidson and Trumbore, 1995). The soil CO₂
9 gradient technique based on syringe samples can provide information on CO₂
10 production at different soil depths, but it cannot make continuous measurements of R_s .
11 Moreover, unavoidable biases usually occur owing to (1) disturbances of the soil
12 environment; (2) the gas extraction, storage, transport, and measurement processes; and
13 (3) the calibration for changes in porosity with soil depth (see review by Baldocchi et
14 al. 2006). Since Hirano et al. (2003), Tang et al. (2003) and Liang et al. (2004) first
15 introduced a modified soil CO₂ gradient technique by using small solid-state NDIR CO₂
16 sensors buried in the soil to deduce soil respiration, the technique has been gaining
17 popularity rapidly because it allows to continuously measure R_s with minimal
18 disturbance to the natural soil structure upon installation (e.g., Jassal et al., 2005;

Baldocchi et al., 2006; Vargas and Allen, 2008c; Pingintha et al., 2010). Recently, the modified gradient technique proved that it could provide useful biometeorological signals for analysis of ecosystem processes at time scales of hours, days, weeks, months, and years (Vargas et al., 2010).

The objectives of this study were to (1) compare the seasonal patterns of soil CO₂ effluxes in a larch forest obtained with a multi-channel automated chamber system and a soil CO₂ concentration gradient measurement system; (2) evaluate the suitability of these two systems as standard protocols for soil CO₂ efflux measurement; and then (3) determine the major environmental and biological factors that control the soil CO₂ efflux in this larch forest.

2 Site description

The study site was the Tomakomai flux site (lat 42°44'N, long 141°31'E; elevation, 125 m) in Tomakomai National Forest, southern Hokkaido, Japan. This site is one of the core sites of AsiaFlux network. The altitude of the site is 125 m and the terrain is essentially flat with a gentle slope of 1–2°.

2.1 Vegetation characteristics

The forest is a 45-year-old Japanese larch (*Larix kaempferi* Sarg.) plantation, interspersed with naturally generated Japanese spruce (*Picea jezoensis* Sieb. et Zucc.) and mixed broad-leaved species (*Betula* spp.). In 2001, the stand density was 1087 stems ha⁻¹ and the total basal area was 23.2 m² ha⁻¹, of which larch accounted for 81%. The forest canopy was about 15 m in height, and the overstory canopy leaf area index (LAI) reached 3.1 during the peak of the growing season. The forest floor was densely covered with perennial buckler fern (*Dryopteris crassirhizoma*) but lacked other understory species and moss. In late June, the average height, biomass, and LAI of the understory were 0.5 m, 1.24 t ha⁻¹, and 2.1, respectively. However, leaves of the fern began to fall in the middle of November, and the soil was covered by snow from 0.6 to 1.0 m deep from the end of December to early April.

2.2 Climate

Climate records between 1979 and 2000 from two weather stations about 10 km around the study site, Tomakomai and Shikotsuko, showed that the mean annual precipitation was approximately 1501 mm, and the mean annual temperature was 7.1 °C, with the mean monthly temperature ranging from -4.5 °C in January to 19.8 °C in August (<http://www.data.jma.go.jp/obd/stats/etrn/index.php>).

2.3 Soil characteristics

The soil is a homogeneous, well-drained, arenaceous soil developed from volcaniclastic sediment derived from a volcanic eruption that occurred about 300 years ago. It is classified as an immature Volcanogenous Regosol. There is sparse compacted till at a depth of 0.15–0.20 m. The litter layer (Oie) is 0.01–0.02 m thick and overlies a 5- to 10-cm-thick organic layer containing many fine roots. Beneath this, there is a layer composed of fragments of porous pumice stone (0.005–0.03 m in diameter) with some coarse roots. Over 90% of the root biomass is in the top 0.20-m-thick soil layer, and the estimated total root biomass is 13.1 t ha⁻¹. As a result, the soil is weakly acidic (pH 5.0–6.0) and poor in nutrients. Total soil organic carbon (SOC) and nitrogen storage are about 26.3 t C m⁻³ and 200 g N m⁻³, respectively, and about 90% of SOC is estimated to be in the surface layer between 0–0.30 m (Sakai et al., 2007).

3 Soil CO₂ efflux measurements

3.1 Improved automated chamber system

Liang *et al.* (2003) designed a multi-channel automated chamber system that applied a steady-state technique to the measurement of R_s throughout the four seasons. However,

the pressure inside the chamber was 0.22 Pa higher than that outside the chamber, which is likely to lead to underestimation of the actual R_s (Fang and Moncrieff, 1998). Therefore, we have modified and improved this system using a flow-through, non-steady-state design. In brief, the system comprises a control unit that is contained within a water-proof field access case (0.70 m long \times 0.50 m wide \times 0.35 m high), and 8 to 24 automated chambers. The main components of the control unit are an IRGA (LI-840; LI-COR, Lincoln, NE, USA), a datalogger (CR10X, Campbell Scientific Inc., Logan, UT, USA), a gas sampler, and an air compressor (Fig. 1). The automated chambers (0.9 m long \times 0.9 m wide \times 0.5 m tall) are constructed of clear PVC (1 mm thick) glued to a frame constructed from plastic-coated steel pipe (30-mm square cross-section) (Fig. 2a). Between measurements, the two sections of the chamber lid are raised to allow precipitation and leaf litter to reach the enclosed soil surface, thus keeping the soil conditions as natural as possible. The chamber lids are raised and closed by two pneumatic cylinders (SCM-20B, CKD Corp., Nagoya, Japan) at a pressure of about 0.2 MPa (Fig. 2a), which is generated by a micro-compressor (M-10, Hitachi Ltd., Tokyo, Japan; Fig. 1). During the measurement, the chamber is closed and the chamber air is mixed by two micro-blowers (MF12B, Nihon Blower Ltd., Tokyo, Japan). The chamber air is circulated through the IRGA by a micro-diaphragm pump (5

1 L min⁻¹; CM-50, Enomoto Ltd., Tokyo, Japan), and the CO₂ concentration is monitored
2 by the IRGA. The average power consumption of the whole system is 13 W; thus, the
3 system can be continuous driven by three 75-W solar cells with three 100-A·h
4 deep-cycle batteries.

5 In June 2002, we installed 16 chambers at Tomakomai flux site, at randomly
6 chosen positions on the forest floor within a circular area 40 m in diameter (Fig. 2a).
7 The 16 chambers were divided into two groups, each with 8 chambers. The first group
8 of chambers was used to measure the total soil CO₂ efflux (R_s), and the understory
9 vegetation inside the chambers was clipped periodically during the growing season.
10 Since the major understory species (fern) dies off once the vegetative point is clipped in
11 the growing season, the chambers were installed between individual fern plants. The
12 second group (8 chambers) was used for measuring heterotrophic respiration (R_h), and
13 the chambers were installed in 1 × 1 m root exclusion plots. Trenches 0.005 to 0.01
14 m-wide and 0.50 m deep were dug along the plot boundaries with a root-cutting
15 chainsaw (CSVN671AG, Kioritz Co. Ltd., Tokyo, Japan) and then PVC sheets (4 mm
16 thick) were installed in the trenches to a depth of 0.50 m to prevent the growth of roots.

17 Over the course of an hour, the 16 chambers were closed sequentially by a
18 home-made relay board controlled by the datalogger (Fig. 1). We set the sampling

period for each chamber to 225 s. Therefore, the chambers were open 94% of the time: during each 1-h cycle they were open for 56.3 minutes and closed for 3.7 minutes. Thus, most of the rainfall and leaf litter could enter the chambers, and the interior of each chamber had good exposure to any atmospheric turbulence. Soil temperature at 0.05 m depth and volumetric soil moisture (CS615, Campbell Scientific) at 0.10 m depth inside each chamber were recorded by coupling the datalogger with multiplexers (AM25T, Campbell Scientific). Moreover, air pressure at 0.30 m height at the center of the measurement plot was monitored with a pressure transducer (PX2760, Omega Engineering, Inc., Stamford, CT, USA). The datalogger acquired outputs from the IRGA and the other sensors at 1-s intervals and recorded the averaged values every 5 s. Soil CO₂ efflux (R_s , $\mu\text{mol m}^{-2} \text{s}^{-1}$) was calculated with equation (1)

$$R_s = \frac{VP(1-W)}{RST} \frac{\partial C}{\partial t}, \quad (1)$$

where V is the effective chamber-head volume (m^3), S is the measured soil surface area (m^2), P is the air pressure (hPa), T is the air temperature (K), and W is the water vapor mole fraction (mmol mol^{-1}) inside the chambers; $\partial C/\partial t$ is the initial rate of change in the CO₂ mole fraction ($\mu\text{mol mol}^{-1} \text{s}^{-1}$), and R is the gas constant ($8.314 \text{ Pa m}^3 \text{ K}^{-1} \text{ mol}^{-1}$). Note that the pressure is not the pressure inside the IRGA cell but the pressure inside the chambers and we assumed that there was null pressure difference between the inside

and outside of the chambers.

3.2 Modified soil CO₂ concentration gradient system

In this study, we modified a soil CO₂ gradient system intended for long-term continuous measurements of R_s (Hirano et al., 2003; Liang et al., 2004; Tang et al., 2003). Briefly, we installed the solid-state CO₂ sensors (18.5 mm diameter, 155 mm long) of IRGAs (GMT222, Vaisala, Helsinki, Finland) at four depths to directly measure soil CO₂ concentration profiles. However, there are several negative aspects of applying the Vaisala CO₂ sensors: (1) non-automatic correction of CO₂ concentration for changes in temperature, pressure, particularly humidity inside the cell, (2) heating of the soil when the sensor is activated constantly (Liang et al. 2004; Baldocchi et al. 2006), and (3) difficulty in estimation of an accurate diffusion coefficient (Pinging et al. 2010).

3.2.1 Water vapour sensitivity of the Vaisala CO₂ sensors

To ensure quality measurements, we conducted a set of laboratory experiments. (1) We enclosed a beaker with a polytetrafluoroethylene (PTFE) sheet (TB-1419, Sumitomo Electric Fine Polymer Corp., Osaka, Japan), and sank it in the water to 0.2 m depth. After 24 hours, we discovered that the weight of the beaker did not change (i.e., the

PTFE excluded liquid water entering the beaker). (2) We enclosed one of the two humidity and temperature probes (HMP45D, Vaisala) with the PTFE sheet and inserted them into a plastic case that dried with silica gel for several minutes until the reading of relative humidity was about 4%. We then suddenly removed the two probes and inserted them into another case with its bottom was filled with pure water, which was assumed near the condition that inside the soil. We detected that relative humidity reading from the PTFE enclosed probe increased steadily but lagged by about 125 seconds compared to the bared probe (Fig. 3). These results demonstrate that the PTFE can allow water vapour to diffuse freely across it. (3) We firstly calibrated the Vaisala CO₂ sensors and the LI-840 IRGA at relative humidity of about 17% against gas standards (Nissan Tanaka Corp., Iruma-gun, Saitama, Japan). The agreement between outputs of the Vaisala CO₂ sensors and the LI-840 IRGA was extremely high ($R^2 = 0.9997$; Fig. 4a). The sensors were then calibrated again by the same procedure as above but at relative humidity of about 90%. Compared with the LI-840 IRGA, the bias of the Vaisala CO₂ sensors could be as high as 60 to 100 ppm at calibration standard of 3000 ppm (Fig. 4b). The result indicates that accuracy of the Vaisala CO₂ sensor is significantly dependent on moisture. (4) With the PTFE socks, delay in output of the Vaisala CO₂ sensors occurred about 56 seconds after the LI-840 IRGA (Fig. 5). We infer from our data that

1 this delay was not correlated with moisture (data not shown).

3 **3.2.2 Sensor preparation**

4 To eliminate the errors, we took the following preparatory measures: (1) To prevent
5 damage by rainwater, we enclosed the sensors in PTFE socks. (2) To measure CO₂
6 concentrations at only specific soil depths, we enclosed the sensors in clear PVC (inner
7 diameter 22 mm) casings. (3) We covered the opening at the bottom end of the casing
8 with a fine (0.5 mm) mesh stainless steel screen to prevent soil particles from entering
9 the casing but to allow CO₂ molecules to diffuse into the sensor for measurement of the
10 CO₂ concentration. (4) We setup a thermocouple (T-type) sensor in each one of the
11 sensor casing for monitoring temperature. And (5) we installed a tubing (inner diameter
12 2.5 mm) to each of the sensor casing for measuring the pressure by using a low-cost but
13 high precision pressure transmitter (MPX4115, FreeScale Semiconductor, Austin, Texas,
14 USA).

16 **3.2.3 Field application**

17 In June 2002, we installed two sets of sensors at two locations 0.60 m apart at the
18 Tomakomai site. Because of the shallowness of the soil at this site, we set four sensors

at each location at 0, 0.02 (measurement range of 0-2000 ppp), 0.11 and 0.13 m depths (measurement range of 0-10000 ppm). We defined 0 m depth as the soil surface under the surface litter layer. To minimize soil disturbance, we installed the sensors vertically (Fig. 2b). To avoid heating of the soil adjacent to the probe by the infrared lamp inside the probe (Baldocchi et al., 2006), all probes in this study were powered on at 24 minutes past the top of the hour. After the probes were powered on, they were allowed to warm up for 5 min before their output was recorded with a datalogger (CR10X, CSI) through an AM25T multiplexer at 10-s intervals over the next 2 min. The temperature and pressure inside the sensor casing were recorded simultaneously. Then the probes were powered off until 24 min past the next hour (also see Liang et al. 2004). Soil temperature at 0.02, 0.05, 0.10 and 0.15 m depth and volumetric soil moisture at 0.10 m depth were also recorded at each location. The probes were removed for drying and calibration every two months.

3.2.4 Soil CO₂ efflux calculation

Firstly, the CO₂ concentration recorded from the sensors was corrected for variations in temperature and pressure accordingly to the manufacturer's instruction (Vaisala) and CO₂ molar density ($\mu\text{mol m}^{-3}$) was calculated using the universal gas law. Then, the

CO₂ efflux from the forest floor was computed with Fick's law using concentrations measured at the surface and at 0.02 m depth, under the assumption that the soil was horizontally homogeneous:

$$R_s = -D_s \frac{\partial C}{\partial z} \quad (2)$$

where R_s is the interlayer soil CO₂ efflux ($\mu\text{mol m}^{-2} \text{s}^{-1}$), D_s ($\text{m}^2 \text{s}^{-1}$) is the gaseous CO₂ diffusion coefficient, and $\partial C/\partial z$ is the vertical CO₂ density gradient ($\mu\text{mol m}^{-4}$). D_s was calculated using Campbell's function (Campbell, 1985)

$$D_s = D_0 B \left(\frac{T_{\text{soil}} + 273.15}{273.15} \right)^{1.75} \left(\frac{1013}{P_s} \right), \quad (3)$$

where D_0 is the CO₂ diffusion coefficient in air ($1.39 \times 10^{-5} \text{ m}^2 \text{s}^{-1}$) at 1013 hPa and 273.15 K, T_{soil} is the average soil temperature ($^{\circ}\text{C}$) at 0.02 m depth, and P_s is the air pressure (hPa) inside the sensor casing. B is the relative soil gaseous diffusion coefficient, which was estimated from the air-filled porosity based on the linear relationship between these two parameters. Several empirical models can be used to determine B (Moldrup et al., 2004). Pingintha et al. (2010) recently applied six models and found that soil gradient method overestimated R_s by 90% (ranging from 3% to 173%) compared with the chamber technique (LI-8100, Li-Cor). On the other hand, our earlier study at the Tomakomai site demonstrated that R_s showed only a weak correlation with soil moisture (Liang et al. 2004). Thus, we extrapolated B from

air-filled porosity that was determined in the laboratory by the diffusion chamber method in undisturbed soil cores as the residual of the volume fraction of solid and water (Currie, 1960). More details on the estimation of D_s are given by Hirano et al. (2003).

4 Data analysis

The high-frequency data were analyzed as follows: (1) Individual chambers were used as the statistical units for analyzing spatial variation in soil CO₂, which was quantified by the coefficient of variation (CV). (2) Measurements of the eight chambers used for each process (soil CO₂ efflux and heterotrophic respiration) were averaged to obtain the mean efflux. (3) A *t*-test was used to analyze statistically the difference in magnitude of soil CO₂ effluxes measured by the two approaches. (4) To examine the temperature response of the soil CO₂ efflux, we performed a regression analysis using the temperature response function with data obtained by both the chamber and gradient approaches:

$$R_s = a e^{bT_{\text{soil}}}, \quad (4)$$

where R_s is the CO₂ efflux at soil temperature T_{soil} at a depth of 0.05 m, a is the efflux at 0 °C (i.e., the basal rate), and b is the sensitivity of the soil CO₂ efflux to temperature. The value of b was also used to calculate the Q_{10} coefficient:

$$Q_{10} = e^{10b} , \quad (5)$$

which is the relative increase in the soil CO₂ efflux with a 10 °C increase in soil temperature.

Chamber technique data were missing for the entire snow-covered period, so data for this entire period were calculated by using Eq. (5) and the soil temperature measured at 0.05 m depth. Root respiration (R_r) was estimated as the soil CO₂ efflux less the heterotrophic respiration ($R_r = R_s - R_h$).

5 Results and Discussion

Because of the high stability of both the chamber and the gradient measurement systems, more than 95% of the datasets were available for estimating of R_s . As this site was influenced mainly by soil temperature (see section 5.4), we used hourly soil temperature data (Fig. 6) and the best-fit parameter values of soil CO₂ efflux (Eq. 4) to derive missing data for estimation of the annual R_s .

5.1 Bias in the annual soil CO₂ efflux

Overall, our results showed that R_s calculated from soil CO₂ profiles were very similar to that measured by the chamber method (Fig. 6). The annual R_s measured by the automated chamber approach was 959 g C m⁻², with 57% contributed by heterotrophic respiration (R_h). In contrast, the annual R_s estimated by the soil CO₂ gradient technique was 1040 g C m⁻², about 8% higher than that determined with the automated chamber system. However, if we derive the annual R_s by using the continuously measured soil temperature values and the Q_{10} functions (the solid lines in Fig. 8), then we obtain annual R_s of 933 and 992 g C m⁻² by the automated chamber and soil CO₂ gradient technique, respectively. The higher values of 59-81 g C m⁻² from the gradient technique could cause differences of about 27-37% in the annual NEP estimate for this forest ecosystem by the micrometeorological method (Hirata et al., 2007). If litter decomposition were taken into account, this difference would be larger because the upper probe of the gradient system was installed under the surface litter layer. However, it is worth noting that the difference between the two measurements falls within the lower bounds reported by, for example, Vargas et al. (2008) and Pingintha et al. (2010), who showed gradient effluxes were about 23% and 90% larger than that of the chamber measurements for a Californian forest and a Georgian cropland, respectively. In contrast,

Baldocchi et al. (2006) reported that gradient estimated effluxes were only 77% of that measured by the chamber system in a Californian semiarid mixed temperate forest.

We attempted to combine the two methods to come up with one dataset for estimating more reliable annual R_s . Compared to the chamber measurement, the gradient result showed a tendency of a litter overestimation for low and medium efflux rates and a little underestimation for high efflux rates (Fig. 7). If the gradient method is considered biased, potential sources of error include: (1) the calculated diffusion coefficient slight overestimated R_s throughout most of measurements (Fig. 7); (2) a delay in the sensor's response time caused by the PTFE socks underestimated the soil CO₂ signals during rainfall events (also see section 5.7). The agreement ($R^2 = 0.812$) between the gradient and the chamber measurements is comparable with that reported from the arid or semi-arid ecosystems with annual precipitation <600 mm (Tang et al., 2003; Baldocchi et al., 2006; Vargas and Allen, 2008a)). However, the correlation is more consistent with the datasets that observed from the humid ecosystems with annual precipitation >1500 mm (Jassal et al., 2005; Vargas and Allen, 2008b; Pingintha et al., 2010), which agrees with our laboratory result that high humidity in the soil will reduce the accuracy of the gradient approach.

In our earlier study, we obtained an annual soil CO₂ efflux of 665 g C m⁻² with a

1 steady-state chamber system at this site in 2001 (Liang et al., 2004). If we ignore
2 temperature and precipitation differences between 2001 and 2003, the bias toward
3 higher values of 294 g C m⁻² of the 2003 chamber system suggests that the positive
4 pressure of 0.22 Pa inside the chamber in the steady-state system may have led to
5 underestimation of the soil CO₂ efflux by about 36%. The results are consistent with
6 those of previous laboratory tests that a pressure difference of a few tenths Pa will cause
7 several-fold variation in measured soil CO₂ efflux (Fang and Moncrieff, 1998; Widen
8 and Lindroth, 2003).

9 Larch forests are widely distributed throughout the Northern Hemisphere (e.g.,
10 >40% of Russian forests) and are thus a globally important forest biome. Our results
11 indicate that regional and global terrestrial carbon budget are probably significantly
12 over- or underestimated by upscaling the soil CO₂ data obtained by a single-method
13 approach.

14 15 **5.2 The significance of soil efflux during the snow-covered season**

16 Hirano (2005) used small solid-state CO₂ sensors for *in situ* measurements of soil CO₂
17 concentration profiles, and found that R_s under a snowpack showed a definite seasonal
18 pattern; they were relatively constant between the beginning of winter and midwinter,

but increased dramatically in late winter as the snow melted. In the present study, using the soil temperature-dependent efflux equation (Eq. 4), we estimated the total R_s during the snow-covered period (between 12 December and 17 April) to be 105 g C m^{-2} by the chamber technique, which corresponds to about 11% of the annual R_s . Over the same period, however, we calculated R_s as about 73 g C m^{-2} by the soil CO_2 gradient approach. A bias toward lower values by 32 g C m^{-2} for the gradient approach compared to the chamber technique contributed only about 3% of averaged annual R_s (1000 g C m^{-2}), however it could cause a difference of about 15% in the annual NEP for this forest ecosystem (Hirata et al., 2007). In contrast about 80 g C m^{-2} of R_s in the snow-covered season by the chamber method could be indeed derived from the gradient measurement by using the best fitted equation ($R_{s\text{-chamber}} = 1.049 \cdot R_{s\text{-gradient}}^{0.918}$, $R^2 = 0.812$) in figure 7. While this derivative can reduce the bias in the winter season, the bias of annual R_s between the chamber and gradient measurement will be enhanced. (Brooks et al., 2005) also demonstrated that the failure to account for the winter soil efflux would, on average, result in an overestimation of annual NEP by 71% in deciduous forests and 111% in coniferous forests in the Colorado Rockies.

A few studies have demonstrated that both fungal (Schadt et al., 2003) and bacterial (Lipson et al., 2000) biomass values are higher in snow-covered soils than in the same

soils in summer, suggesting that CO₂ production continues throughout the snow-covered period and constitutes an important part of the annual carbon budget in snowy ecosystems. Our data suggest that the gradient approach is a practical means to continuously measure R_s during snow-covered season, however the results need to be farther validated due to that the Vaisala's IRGA was not temperature assured (e.g., LI-840 IRGA was always warmed-up at 50°C). More intensive intercomparison studies of chamber, soil CO₂ gradient, and micrometeorological techniques might clarify the bias in soil CO₂ efflux measurements between the chamber and soil CO₂ gradient techniques.

5.3 Temporal and spatial variations in the soil CO₂ efflux

Soil CO₂ effluxes measured by both the automated chamber system and the soil CO₂ gradient system showed notable seasonal patterns (Fig. 6). During the snow-covered season, between 9 December and 17 April, soil CO₂ efflux measured by the soil CO₂ gradient technique averaged 0.57 $\mu\text{mol m}^{-2} \text{s}^{-1}$, and ranged from 0.40 to 0.70 $\mu\text{mol m}^{-2} \text{s}^{-1}$ (Fig. 6c). Over the same period, R_s was estimated to be $0.83 \pm 0.03 \mu\text{mol m}^{-2} \text{s}^{-1}$ by the chamber measurement by using the Eq. 4 (Fig. 6b). The only slight variation in estimated R_s during the snow-covered season may be explained by the fact that soil

1 temperature ($-0.3 \pm 0.3^{\circ}\text{C}$) showed high stability under the snowpack (Fig. 6a). After the
2 snow melted, the soil CO_2 efflux increased exponentially until day 180 as the soil
3 temperature increased and soil moisture decreased. The soil CO_2 efflux remained high
4 during the summer (between days 180 and 260), on average 5.5 and $6.5 \mu\text{mol m}^{-2} \text{s}^{-1}$ as
5 measured by the automated chamber system and soil CO_2 gradient system, respectively.
6 Then, it decreased steadily with the decreasing soil temperature until the soil was
7 covered by the snow (Fig. 6). These results are consistent with those that we reported in
8 our earlier study (Liang et al., 2004).

9 The soil CO_2 efflux varied spatially; the coefficient of variation (CV) of the soil CO_2
10 efflux was 21% and the heterotrophic respiration CV was 20% that estimated from the
11 chamber measurement. Spatial variations in the CO_2 efflux are often observed between
12 measurement plots separated by only a few centimeters, reflecting rock sizes,
13 disturbances by soil fauna, pockets of fine root proliferation, and remnants of decaying
14 organic matter (Davidson et al., 2002; Liang et al., 2004). Furthermore, spatial variation
15 in the soil CO_2 efflux depends on the size of the chamber used for the measurement. In
16 the same forest stand as that used for this study, Liang et al. (2004) reported CVs as
17 high as 44% for data obtained with a standard LI-COR soil chamber (LI-6400-09; 15
18 plots) with a surface area of 0.0081 m^2 . In contrast, the CV decreased to 30% when the

1 chamber area was increased to 0.071 m² (16 plots), and they obtained a low CV of 16%
2 when the chamber area was 0.81 m² (8 plots). Therefore, Liang et al. (2004) concluded
3 that, for studying spatial variations in soil CO₂ efflux, a system composed of a smaller
4 number of larger chambers would better characterize a site with less labor.

5 On the other hand, we were unable to estimated the soil efflux CV from the
6 gradient approach and because of the cost of sensors we could not conduct more
7 measurement replications in a desired manner.

9 **5.4 Responses of the soil CO₂ efflux to soil temperature and moisture**

10 Temperature is the most commonly studied environmental control on soil CO₂ efflux
11 (Lloyd and Taylor, 1994; Davidson and Janssens, 2006; Zhou et al., 2009). We
12 developed functions to evaluate the effect of soil temperature on soil CO₂ effluxes (Fig.
13 8) by fitting an exponential curve to the relationship between efflux and soil
14 temperature data obtained over the same measurement period (between days 108 and
15 345). We also calculated Q_{10} coefficients to determine the apparent temperature
16 sensitivity of the soil CO₂ efflux, obtaining values of 3.1 and 4.5 by the chamber and
17 gradient technique, respectively (Fig. 8a, c). Our Q_{10} values were significantly higher
18 than the global mean soil respiration Q_{10} value (ranging 1.43-2.03; Raich et al., 2002;

Zhou et al., 2009). Generally, Q_{10} varies between 1 and 5 and is negatively correlated with temperature and positively correlated with soil moisture (Lloyd and Taylor, 1994). Therefore, we attributed the high Q_{10} values obtained in this study mainly to the high soil moisture (ranging between 25 and 55% with 95% confidence interval of 30-40%) at this site and the relatively low average annual temperature (7.1°C). The higher Q_{10} obtained by the gradient technique than by the chamber technique can be attributed to the systematically higher effluxes observed by the gradient technique during the growing season and the lower effluxes observed during the non-growing season (November and December) compared with effluxes observed by the chamber technique.

Soil CO₂ efflux is also controlled by moisture availability. In the present study, to reduce the confounding effect of temperature and evaluate the role of soil moisture on the soil CO₂ efflux, we plotted the temperature-normalized efflux (i.e., the ratio of the observed soil CO₂ efflux to the temperature-fitted efflux) against the volumetric soil moisture (Fig. 9). Temperature-normalized efflux values were around 1.0 throughout the measurement period, and the low correlation coefficients ($R^2 < 0.05$) and gradual slopes (≤ 0.01) of the regression lines indicate that soil CO₂ effluxes at Tomakomai forest were not sensitive to soil moisture over a wide range of field conditions (with volumetric soil moisture ranging between 25 and 55%; Fig. 9). The high sensitivity of soil respiration to

soil temperature and its low sensitivity to moisture at this site is consistent with the findings of studies conducted in relative humid forest ecosystems (Tang et al., 2008; Ruehr et al., 2010; Klimek et al., 2009).

5.5 Seasonal variation of the soil CO₂ efflux Q_{10} coefficient

To investigate the mechanism by which temperature affects the soil efflux, we estimated the Q_{10} coefficient from monthly data sets obtained by the automated chamber system. Figure 6 shows the seasonal changes in Q_{10} values for root respiration, heterotrophic respiration, and the total soil CO₂ efflux in 2003.

The Q_{10} of root respiration peaked in June when productivities of fine roots and the rhizosphere were highest, suggesting that root respiration is controlled mainly by canopy processes (e.g. photosynthesis) through metabolism of recently fixed carbohydrates (Tang et al., 2005; Moyano et al., 2008; Sampson et al., 2007; Irvine et al., 2008; Baldocchi et al., 2006; Yuste et al., 2004; Hasselquist et al., 2010). The lowest root respiration Q_{10} was observed in August, during the hottest part of the summer. In contrast, Q_{10} values of heterotrophic respiration remained relatively constant (at around 3.0) across the growing season but increased dramatically from late autumn (October) to early winter (December), accompanied by an extreme decrease in temperature.

Precipitation was abundant in the Hokkaido region and no evidence for seasonal drought was observed. Thus, the different seasonality of Q_{10} between root respiration and heterotrophic respiration suggests that the temperature response of root respiration has a different mechanism from that of heterotrophic respiration; when environmental conditions (i.e., temperature and moisture) are favorable for microbial activity, heterotrophic respiration contributes more to the total soil CO₂ efflux, and when they are favorable for photosynthesis and root growth, root respiration contributes more. The Q_{10} values of root respiration and heterotrophic respiration averaged over the growing season were 2.8 and 3.4, respectively. Lower Q_{10} of root respiration than of heterotrophic respiration in this larch forest does not agree with the report for a temperate mixed forest at the Harvard Forest, in which the Q_{10} value of root respiration (4.6) was significantly greater than that of soil heterotrophic respiration (2.5) (Boone et al., 1998). Our finding suggests that the high temperature sensitivity of heterotrophic respiration will offset the forest carbon sequestration in the changing world with elevated atmospheric CO₂ concentration (Bond-Lamberty and Thomson, 2010).

There is increasing evidence that Q_{10} of soil CO₂ efflux is not seasonally constant and tends to increase with decreasing temperature and increasing soil moisture (Chen et al., 2009a). Recent field studies have also observed significant seasonal changes in Q_{10}

values of the soil CO₂ efflux (Chen et al., 2009a; Liu et al., 2006b; Phillips et al., 2010; Xu and Qi, 2001; Janssens and Pilegaard, 2003). By partitioning soil CO₂ efflux into root respiration and heterotrophic respiration, we showed that the seasonality of the soil CO₂ efflux Q_{10} value was similar to that of the root respiration Q_{10} (Fig. 10), a finding consistent with previous report about the total soil CO₂ efflux, in which Janssens and Pilegaard (2003) suspected that low summertime Q_{10} values were caused by summer drought stress. The similar seasonality that we found between the root respiration Q_{10} and the total soil CO₂ efflux Q_{10} suggests that large seasonal changes in root respiration dominate the seasonal pattern of the soil CO₂ efflux, especially during the growing season. However, the relative stability of the heterotrophic respiration Q_{10} is consistent with both laboratory results and theoretical predictions (Davidson and Janssens, 2006). The seasonal Q_{10} variation indicates that a Q_{10} function (e.g., Eq. 5) based on annual data will under- or overestimate the soil CO₂ efflux on shorter timescales; thus, empirical models should be parameterized at a time resolution similar to that required by the output of the model.

5.6 Root respiration and heterotrophic respiration

Distinguishing root respiration from heterotrophic respiration is an important first step

1 in interpreting measurements and modeling, as autotrophic and heterotrophic respiration
2 can respond differently to the environment and to environmental disturbances (Ryan and
3 Law, 2005; Cisneros-Dozal et al., 2007; Moyano et al., 2008; Irvine et al., 2008). In this
4 larch forest, the relative contributions of root respiration and heterotrophic respiration to
5 the total soil CO₂ efflux showed distinct seasonal patterns (Fig. 11), consistent with the
6 suggestion of Hanson et al. (2000) that the proportion of the soil CO₂ efflux derived
7 from root and heterotrophic respiration may vary seasonally and among ecosystems.

8 Heterotrophic respiration accounted for most of the soil CO₂ efflux (65–70%)
9 between 30 April and 9 June (days 120 to 160), probably because the rapid increase in
10 soil temperature in the spring after the snow melted enhanced decomposition of the
11 recently accumulated litterfall, as well as because the decreasing soil moisture led to
12 increased oxygenation, which stimulated microbial activity. As a result, the contribution
13 of heterotrophic respiration to the total efflux increased and that of autotrophic
14 respiration decreased. Once the canopy began to leaf out, from 25 May (days 145),
15 photosynthesis increased exponentially and was maintained at a high rate, presumably
16 providing substrate for root and associated rhizosphere respiration, which eventually
17 matched or exceeded the contribution of heterotrophic respiration (Vargas et al., 2010;
18 Tang et al., 2005; Moyano et al., 2008; Hasselquist et al., 2010). Thus, autotrophic

1 respiration contributed more (around 50%) to the soil CO₂ efflux between 10 June and 3
2 August (days 161 to 215), when the plants were growing rapidly. In midsummer, from
3 early August to mid-September (days 216 to 258), high temperatures probably both
4 inhibited photosynthesis and enhanced decomposition of litterfall, allowing the
5 heterotrophic contribution to reach a second peak. As the temperature decreased from
6 the beginning of September, the heterotrophic respiration contribution decreased but the
7 contribution from root respiration remained at a relatively high level owing to the higher
8 allocation of photosynthate (i.e., starch) to the roots and ectomycorrhizal fungi (Liang et
9 al., 2004; Liu et al., 2006a; Kurganova et al., 2007; Hasselquist et al., 2010).

10 During the whole growing season, between 15 May (day 135) and 15 October (day
11 288), the average contribution of heterotrophic respiration to the total soil CO₂ efflux
12 was 57%. During the non-growing season, root respiration and heterotrophic respiration
13 each accounted for roughly half of the soil CO₂ efflux. Hanson *et al.* (2000) reviewed
14 that, in forests, heterotrophic contributions were ranging from 40% during the growing
15 season to 54% annually. The root exclusion method (trenching) used in this study to
16 distinguish autotrophic from heterotrophic respiration might overestimate heterotrophic
17 respiration in the short term (e.g., within the first treatment year) owing to the
18 decomposition of dead roots, but it might underestimate heterotrophic respiration in the

long term (e.g., over one year) because no new fine root litter is supplied.

5.7 Impact of rainfall events on the soil CO₂ efflux

Several studies have detected large ecosystem respiration pulses during pulse rain events in arid ecosystems (Lee et al., 2004; Xu et al., 2004; Liang et al., 2003; Liang et al., 2004; Irvine et al., 2005; Kelliher et al., 2004; Chen et al., 2009b; Inglema et al., 2009; Baldocchi et al., 2006). In this study, both the automated chamber and soil CO₂ gradient approaches revealed episodic emissions (Fig. 6b, c); R_s increased by approximately 70% following rain events with >20 mm of precipitation (Fig. 6b). R_s responded rapidly and instantaneously to the onset of rain and returned to the pre-rain rate several hours after the rain had stopped. Our results are consistent with the findings of rain simulation studies (Lee et al., 2004; Chen et al., 2009b), and field observations (Inglema et al., 2009; Xu et al., 2004; Baldocchi et al., 2006). A 170-mm rainstorm has been reported to enhance the soil CO₂ efflux up to fivefold, and the efflux returns to the pre-rain value usually <1 h after the rain has stopped, showing no sign of a post-wetting efflux pulse (Lee et al., 2004). Kelliher et al. (2004) reported that in a young ponderosa pine forest, soil CO₂ efflux increased threefold with a simulated rain event that increased the soil water holding capacity of previously dry soil to 60%, and then it

1 returned to pre-watering levels within 24 h of the pulse event. However, automated
2 chamber measurements in the same forest (Irvine and Law, 2002) showed that the
3 intensity of rain events had a substantial effect on interannual variation in soil
4 respiration because heavy rain events resulted in prolonged elevation of the soil CO₂
5 efflux (e.g., 7 days).

6 The rapid response of the soil CO₂ efflux to pulse rain events suggests that
7 continuous measurements by both the automated chamber and soil CO₂ gradient
8 systems are important for accurate, quantitative estimates of the contribution of the soil
9 CO₂ efflux to the carbon balance in a particular ecosystem(Vargas et al., 2010). Periodic
10 manual chamber measurements made only under fine-weather conditions undoubtedly
11 underestimate soil CO₂ effluxes in rainy weather because the soil CO₂ pulse signals are
12 missed, which may strongly affect the estimated ecosystem carbon balance (Lee et al.,
13 2004; Xu et al., 2004; McCulley et al., 2007). For instance, if we derive the parameters
14 of a soil temperature-dependent Q_{10} function (Eq. 5) using the CO₂ efflux values and
15 soil temperatures observed only on the fine days (daily rainfall = 0 mm) of this study
16 and then apply them to rainy days (daily rainfall \geq 1 mm), then the estimated annual soil
17 CO₂ efflux decreases by 24 g C m⁻², accounting for only about 2% of annual soil CO₂
18 efflux but probably underestimating NEP for about 11% in this larch ecosystem (Hirata

et al., 2007).

6 Conclusions

There has been a growing interest in the role of ecosystems in the global carbon cycle, particularly the response and feedback of soil CO₂ efflux to the rapid changing climate system. However, soil CO₂ efflux processes are complex because the interactions between climatic forcing and biological components act at multiple temporal and spatial scales. To better understand the abiotic and biotic factors that control soil CO₂ efflux, we developed two systems for continuous (hourly) and accurate measurement of soil CO₂ effluxes: a multi-channel automated soil chamber system usable only during snow-free periods, and a soil CO₂ concentration gradient system, which can be used throughout the year, even when the ground is snow-covered.

(1) Annual soil CO₂ effluxes of 959 and 1040 g C m⁻² were obtained with the automated chamber system and by the soil CO₂ gradient technique, respectively.

While the bias of 81 g C m⁻² between the two measurements corresponds to about 8% of the annual mean R_s , this error falls within the lower bounds reported from the previous studies.

(2) The automated chamber system has the advantages of being able to

1 simultaneously partition soil CO₂ efflux into autotrophic (root) and heterotrophic
2 components and evaluate their temporal and spatial variations. With the
3 chamber-based measurements, the estimated annual mean contribution of
4 heterotrophic respiration to the soil CO₂ efflux was about 57%.

5 (3) The gradient system can provides the vertical information of CO₂ production
6 and transport at different soil depths. The successful monitoring of soil CO₂
7 concentration profiles under the snowpack suggests that the gradient approach
8 cab be a practical means for continuous calculating soil CO₂ efflux. The good
9 agreement between the CO₂ gradient and soil chamber system ($R^2 = 0.812$)
10 results indicates the former can be ued for inter-gap-filling of the missing data of
11 the latter, especially for deriving the missing measurement during the
12 snow-covered season.

13 (4) The relatively high Q_{10} values (between 3.1 and 4.5) and the low moisture
14 sensitivity of the soil CO₂ efflux demonstrated that temperature was the most
15 importance environmental factor driving the soil CO₂ efflux in this forest.

16 (5) We detected a large seasonality of soil CO₂ efflux Q_{10} and discovered that the
17 root respiration Q_{10} was dominantly responsible for the seasonal pattern of the
18 soil CO₂ efflux Q_{10} .

(6) The fast-response chamber technique showed that temporarily higher fluxes following rain events were responsible for about 2% of the annual soil CO₂ efflux, suggesting that high-resolution continuous measurements are important for accurate quantitative estimation of the contribution of the soil CO₂ efflux to the ecosystem carbon balance.

(7) Finally, we suggest that new cost-effective sensors can be used for accurate monitoring soil CO₂ concentration and that new models capable of accurately calculating soil gases diffusion coefficient are urgently needed for improving the soil CO₂ gradient technique. Furthermore, additional *in situ* intercomparison investigations (for instance, a field campaign using the eddy covariance measurement method) are essential to validate annual soil CO₂ efflux estimates.

Acknowledgements

We thank Mr. Koh Inukai and Mr. Yasuyuki Kitamori (Econixe, Hokkaido) for their very efficient management of the Tomakomai flux site. We also thank two anonymous reviewers and the handling editor (Joon Kim) for their constructive suggestions to improve this manuscript. This work was supported by the Global Environmental Research Fund (B-073), Ministry of the Environment, Japan. This is a contribution to

the A3 Foresight Program (CarboEastAsia) funded by the Japan Society for the Promotion of Science.

References

Baldocchi, D., Tang, J. W., and Xu, L. K.: How switches and lags in biophysical regulators affect spatial-temporal variation of soil respiration in an oak-grass savanna, *Journal of Geophysical Research-Biogeosciences*, 111, 2006.

Bond-Lamberty, B., and Thomson, A.: Temperature-associated increases in the global soil respiration record, *Nature*, 464, 579-U132, 10.1038/nature08930, 2010.

Boone, R. D., Nadelhoffer, K. J., Canary, J. D., and Kaye, J. P.: Roots exert a strong influence on the temperature sensitivity of soil respiration, *Nature*, 396, 570-572, 1998.

Brooks, P. D., McKnight, D., and Elder, K.: Carbon limitation of soil respiration under winter snowpacks: potential feedbacks between growing season and winter carbon fluxes, *Global Change Biology*, 11, 231-238, 2005.

Campbell, G. S.: *Soil Physics with BASIC: Transport Models for Soil-Plant Systems*, Elsevier, New York, 150 pp., 1985.

Chen, J. M., Huang, S. E., Ju, W., Gaumont-Guay, D., and Black, T. A.: Daily

- 1 heterotrophic respiration model considering the diurnal temperature variability in
2 the soil, *Journal of Geophysical Research-Biogeosciences*, 114, 2009a.
- 3 Chen, S. P., Lin, G. H., Huang, J. H., and Jenerette, G. D.: Dependence of carbon
4 sequestration on the differential responses of ecosystem photosynthesis and
5 respiration to rain pulses in a semiarid steppe, *Global Change Biology*, 15,
6 2450-2461, 2009b.
- 7 Cisneros-Dozal, L. M., Trumbore, S. E., and Hanson, P. J.: Effect of moisture on leaf
8 litter decomposition and its contribution to soil respiration in a temperate forest,
9 *Journal of Geophysical Research-Biogeosciences*, 112, 2007.
- 10 Currie, J. A.: Gaseous diffusion in porous media Part 1. - A non-steady state method,
11 *British Journal of Applied Physics*, 11, 314-317, 1960.
- 12 Davidson, E. A., and Trumbore, S. E.: Gas Diffusivity and Production of Co₂ in Deep
13 Soils of the Eastern Amazon, *Tellus Series B-Chemical and Physical Meteorology*,
14 47, 550-565, 1995.
- 15 Davidson, E. A., Savage, K., Verchot, L. V., and Navarro, R.: Minimizing artifacts and
16 biases in chamber-based measurements of soil respiration, *Agricultural and Forest*
17 *Meteorology*, 113, 21-37, 2002.
- 18 Davidson, E. A., and Janssens, I. A.: Temperature sensitivity of soil carbon

1 decomposition and feedbacks to climate change, *Nature*, 440, 165-173, 2006.

2 Drewitt, G. B., Black, T. A., Nesic, Z., Humphreys, E. R., Jork, E. M., Swanson, R.,

3 Ethier, G. J., Griffis, T., and Morgenstern, K.: Measuring forest floor CO₂ fluxes in a

4 Douglas-fir forest, *Agricultural and Forest Meteorology*, 110, 299-317, 2002.

5 Drewitt, G. B., Black, T. A., and Jassal, R. S.: Using measurements of soil CO₂ efflux

6 and concentrations to infer the depth distribution of CO₂ production in a forest soil,

7 *Canadian Journal of Soil Science*, 85, 213-221, 2005.

8 Fahnestock, J. T., Jones, M. H., and Welker, J. M.: Wintertime CO₂ efflux from arctic

9 soils: Implications for annual carbon budgets, *Global Biogeochemical Cycles*, 13,

10 775-779, 1999.

11 Fang, C., and Moncrieff, J. B.: An open-top chamber for measuring soil respiration and

12 the influence of pressure difference on CO₂ efflux measurement, *Functional*

13 *Ecology*, 12, 319-325, 1998.

14 Friedlingstein, P., Cox, P., Betts, R., Bopp, L., Von Bloh, W., Brovkin, V., Cadule, P.,

15 Doney, S., Eby, M., Fung, I., Bala, G., John, J., Jones, C., Joos, F., Kato, T.,

16 Kawamiya, M., Knorr, W., Lindsay, K., Matthews, H. D., Raddatz, T., Rayner, P.,

17 Reick, C., Roeckner, E., Schnitzler, K. G., Schnur, R., Strassmann, K., Weaver, A. J.,

18 Yoshikawa, C., and Zeng, N.: Climate-carbon cycle feedback analysis: Results from

1 the (CMIP)-M-4 model intercomparison, *Journal of Climate*, 19, 3337-3353, 2006.

2 Gaumont-Guay, D., Black, T. A., McCaughey, H., Barr, A. G., Krishnan, P., Jassal, R. S.,
3 and Nesic, Z.: Soil CO₂ efflux in contrasting boreal deciduous and coniferous stands
4 and its contribution to the ecosystem carbon balance, *Global Change Biology*, 15,
5 1302-1319, 2009.

6 Goulden, M. L., and Crill, P. M.: Automated measurements of CO₂ exchange at the
7 moss surface of a black spruce forest, *Tree Physiol*, 17, 537-542, 1997.

8 Hanson, P. J., Edwards, N. T., Garten, C. T., and Andrews, J. A.: Separating root and soil
9 microbial contributions to soil respiration: A review of methods and observations,
10 *Biogeochemistry*, 48, 115-146, 2000.

11 Hasselquist, N. J., Vargas, R., and Allen, M. F.: Using soil sensing technology to
12 examine interactions and controls between ectomycorrhizal growth and
13 environmental factors on soil CO₂ dynamics, *Plant and Soil*, 331, 17-29,
14 10.1007/s11104-009-0183-y, 2010.

15 Hirano, T., Kim, H., and Tanaka, Y.: Long-term half-hourly measurement of soil CO₂
16 concentration and soil respiration in a temperate deciduous forest, *Journal of*
17 *Geophysical Research-Atmospheres*, 108, 4631, doi:4610.1029/2003JD003766,
18 2003.

- 1 Hirano, T.: Seasonal and diurnal variations in topsoil and subsoil respiration under
2 snowpack in a temperate deciduous forest, *Global Biogeochemical Cycles*, 19,
3 2005.
- 4 Hirata, R., Hirano, T., Saigusa, N., Fujinuma, Y., Inukai, K., Kitamori, Y., Takahashi, Y.,
5 and Yamamoto, S.: Seasonal and interannual variations in carbon dioxide exchange
6 of a temperate larch forest, *Agricultural and Forest Meteorology*, 147, 110-124,
7 2007.
- 8 Hubbard, R. M., Ryan, M. G., Elder, K., and Rhoades, C. C.: Seasonal patterns in soil
9 surface CO₂ flux under snow cover in 50 and 300 year old subalpine forests,
10 *Biogeochemistry*, 73, 93-107, 2005.
- 11 Inglima, I., Alberti, G., Bertolini, T., Vaccari, F. P., Gioli, B., Miglietta, F., Cotrufo, M. F.,
12 and Peressotti, A.: Precipitation pulses enhance respiration of Mediterranean
13 ecosystems: the balance between organic and inorganic components of increased
14 soil CO₂ efflux, *Global Change Biology*, 15, 1289-1301, 2009.
- 15 IPCC: *Climate Change 2007: The Physical Science Basis*, Cambridge Univ. Press.,
16 2007.
- 17 Irvine, J., and Law, B. E.: Contrasting soil respiration in young and old-growth
18 ponderosa pine forests, *Global Change Biology*, 8, 1183-1194, 2002.

- 1 Irvine, J., Law, B. E., and Kurpius, M. R.: Coupling canopy gas exchange with root and
2 rhizosphere respiration in a semi-arid forest, *Biogeochemistry*, (in press), 2005.
- 3 Irvine, J., Law, B. E., Martin, J. G., and Vickers, D.: Interannual variation in soil CO₂
4 efflux and the response of root respiration to climate and canopy gas exchange in
5 mature ponderosa pine, *Global Change Biology*, 14, 2848-2859, 2008.
- 6 Janssens, I. A., Kowalski, A. S., Longdoz, B., and Ceulemans, R.: Assessing forest soil
7 CO₂ efflux: an in situ comparison of four techniques, *Tree Physiology*, 20, 23-32,
8 2000.
- 9 Janssens, I. A., Kowalski, A. S., and Ceulemans, R.: Forest floor CO₂ fluxes estimated
10 by eddy covariance and chamber-based model, *Agricultural and Forest Meteorology*,
11 106, 61-69, 2001.
- 12 Janssens, I. A., and Pilegaard, K.: Large seasonal changes in Q₁₀ of soil respiration in a
13 beech forest, *Global Change Biology*, 9, 911-918, 2003.
- 14 Jassal, R., Black, A., Novak, M., Morgenstern, K., Nesic, Z., and Gaumont-Guay, D.:
15 Relationship between soil CO₂ concentrations and forest-floor CO₂ effluxes,
16 *Agricultural and Forest Meteorology*, 130, 176-192, 2005.
- 17 Jassal, R. S., Black, T. A., Cai, T. B., Morgenstern, K., Li, Z., Gaumont-Guay, D., and
18 Nesic, Z.: Components of ecosystem respiration and an estimate of net primary

productivity of an intermediate-aged Douglas-fir stand, *Agricultural and Forest Meteorology*, 144, 44-57, 2007.

Kelliher, F. M., Ross, D. J., Law, B. E., Baldocchi, D. D., and Rodda, N. J.: Limitations to carbon mineralization in litter and mineral soil of young and old ponderosa pine forests, *For. Ecol. Manage.*, 191, 201-213, 2004.

Klimek, B., Choczynski, M., and Juszkievicz, A.: Scots pine (*Pinus sylvestris* L.) roots and soil moisture did not affect soil thermal sensitivity, *European Journal of Soil Biology*, 45, 442-447, 10.1016/j.ejsobi.2009.06.008, 2009.

Kurganova, I. N., Yermolaev, A. M., de Gerenyu, V. O. L., Larionova, A. A., Kuzyakov, Y., Keller, T., and Lange, S.: Carbon balance in the soils of abandoned lands in Moscow region, *Eurasian Soil Sci.*, 40, 51-58, 2007.

Law, B. E., Ryan, M. G., and Anthoni, P. M.: Seasonal and annual respiration of a ponderosa pine ecosystem, *Global Change Biology*, 5, 169-182, 1999.

Law, B. E., Falge, E., Gu, L., Baldocchi, D. D., Bakwin, P., Berbigier, P., Davis, K., Dolman, A. J., Falk, M., Fuentes, J. D., Goldstein, A., Granier, A., Grelle, A., Hollinger, D., Janssens, I. A., Jarvis, P., Jensen, N. O., Katul, G., Mahli, Y., Matteucci, G., Meyers, T., Monson, R., Munger, W., Oechel, W., Olson, R., Pilegaard, K., Paw, K. T., Thorgeirsson, H., Valentini, R., Verma, S., Vesala, T.,

1 Wilson, K., and Wofsy, S.: Environmental controls over carbon dioxide and water
2 vapor exchange of terrestrial vegetation, *Agricultural and Forest Meteorology*, 113,
3 97-120, 2002.

4 Lee, X.: On micrometeorological observations of surface-air exchange over tall
5 vegetation, *Agricultural and Forest Meteorology*, 91, 39-49, 1998.

6 Lee, X., Wu, H. J., Sigler, J., Oishi, C., and Siccama, T.: Rapid and transient response of
7 soil respiration to rain, *Global Change Biology*, 10, 1017-1026, 2004.

8 Liang, N., Inoue, G., and Fujinuma, Y.: A multichannel automated chamber system for
9 continuous measurement of forest soil CO₂ efflux, *Tree Physiology*, 23, 825-832,
10 2003.

11 Liang, N., Nakadai, T., Hirano, T., Qu, L. Y., Koike, T., Fujinuma, Y., and Inoue, G.: In
12 situ comparison of four approaches to estimating soil CO₂ efflux in a northern larch
13 (*Larix kaempferi* Sarg.) forest, *Agricultural and Forest Meteorology*, 123, 97-117,
14 2004.

15 Lipson, D. A., Schmidt, S. K., and Monson, R. K.: Carbon availability and temperature
16 control the post-snowmelt decline in alpine soil microbial biomass, *Soil Biology &
17 Biochemistry*, 32, 441-448, 2000.

18 Liu, H. S., Li, L. H., Han, X. G., Huang, J. H., Sun, J. X., and Wang, H. Y.: Respiratory

substrate availability plays a crucial role in the response of soil respiration to environmental factors, *Applied Soil Ecology*, 32, 284-292, 2006a.

Liu, Q., Edwards, N. T., Post, W. M., Gu, L., Ledford, J., and Lenhart, S.: Temperature-independent diel variation in soil respiration observed from a temperate deciduous forest, *Global Change Biology*, 12, 2136-2145, 2006b.

Lloyd, J., and Taylor, J. A.: On the Temperature-Dependence of Soil Respiration, *Functional Ecology*, 8, 315-323, 1994.

Luyssaert, S., Schulze, E. D., Borner, A., Knohl, A., Hessenmoller, D., Law, B. E., Ciais, P., and Grace, J.: Old-growth forests as global carbon sinks, *Nature*, 455, 213-215, 2008.

McCulley, R. L., Boutton, T. W., and Archer, S. R.: Soil respiration in a subtropical savanna parkland: Response to water additions, *Soil Sci. Soc. Am. J.*, 71, 820-828, 2007.

Moldrup, P., Olesen, T., Yoshikawa, S., Komatsu, T., and Rolston, D. E.: Three-porosity model for predicting the gas diffusion coefficient in undisturbed soil, *Soil Sci. Soc. Am. J.*, 68, 750-759, 2004.

Moyano, F. E., Kutsch, W. L., and Rebmann, C.: Soil respiration fluxes in relation to photosynthetic activity in broad-leaf and needle-leaf forest stands, *Agricultural and*

1 Forest Meteorology, 148, 135-143, 2008.

2 Phillips, S. C., Varner, R. K., Frolking, S., Munger, J. W., Bubier, J. L., Wofsy, S. C.,
3 and Crill, P. M.: Interannual, seasonal, and diel variation in soil respiration relative
4 to ecosystem respiration at a wetland to upland slope at Harvard Forest, Journal of
5 Geophysical Research-Biogeosciences, 115, 10.1029/2008jg000858, 2010.

6 Pingintha, N., Leclerc, M. Y., Beasley, J. P., Zhang, G. S., and Senthong, C.: Assessment
7 of the soil CO₂ gradient method for soil CO₂ efflux measurements: comparison of
8 six models in the calculation of the relative gas diffusion coefficient, Tellus Series
9 B-Chemical and Physical Meteorology, 62, 47-58,
10 10.1111/j.1600-0889.2009.00445.x, 2010.

11 Raich, J. W., Potter, C. S., and Bhagawati, D.: Interannual variability in global soil
12 respiration, 1980-94, Global Change Biology, 8, 800-812, 2002.

13 Ruehr, N. K., Knohl, A., and Buchmann, N.: Environmental variables controlling soil
14 respiration on diurnal, seasonal and annual time-scales in a mixed mountain forest in
15 Switzerland, Biogeochemistry, 98, 153-170, 10.1007/s10533-009-9383-z, 2010.

16 Ryan, M. G., and Law, B. E.: Interpreting, measuring, and modeling soil respiration,
17 Biogeochemistry, 73, 3-27, 10.1007/s10533-004-5167-7, 2005.

18 Sakai, Y., Takahashi, M., and Tanaka, N.: Root biomass and distribution of a

1 Picea-Abies stand and a Latrix-Betula stand in pumiceous Entisols in Japan, Journal
2 of Forest Research, 12, 120-125, 2007.

3 Sampson, D. A., Janssens, I. A., Yuste, J. C., and Ceulemans, R.: Basal rates of soil
4 respiration are correlated with photosynthesis in a mixed temperate forest, Global
5 Change Biology, 13, 2008-2017, 2007.

6 Savage, K. E., and Davidson, E. A.: A comparison of manual and automated systems for
7 soil CO₂ flux measurements: trade-offs between spatial and temporal resolution,
8 Journal of Experimental Botany, 54, 891-899, 2003.

9 Schadt, C. W., Martin, A. P., Lipson, D. A., and Schmidt, S. K.: Seasonal dynamics of
10 previously unknown fungal lineages in tundra soils, Science, 301, 1359-1361, 2003.

11 Simunek, J., and Suarez, D. L.: Modeling of Carbon-Dioxide Transport and Production
12 in Soil .1. Model Development, Water Resources Research, 29, 487-497, 1993.

13 Sommerfeld, R. A., Mosier, A. R., and Musselman, R. C.: CO₂, CH₄ And N₂O Flux
14 Through A Wyoming Snowpack And Implications For Global Budgets, Nature, 361,
15 140-142, 1993.

16 Takle, E. S., Massman, W. J., Brandle, J. R., Schmidt, R. A., Zhou, X. H., Litvina, I. V.,
17 Garcia, R., Doyle, G., and Rice, C. W.: Influence of high-frequency ambient
18 pressure pumping on carbon dioxide efflux from soil, Agricultural and Forest

1 Meteorology, 124, 193-206, 2004.

2 Tang, J., Baldocchi, D. D., Qi, Y., and Xu, L. K.: Assessing soil CO₂ efflux using
3 continuous measurements of CO₂ profiles in soils with small solid-state sensors,
4 Agricultural and Forest Meteorology, 118, 207-220, 2003.

5 Tang, J., Baldocchi, D. D., and Xu, L.: Tree photosynthesis modulates soil respiration
6 on a diurnal basis, Global Change Biology, (in press), 2005.

7 Tang, J. W., Bolstad, P. V., Desai, A. R., Martin, J. G., Cook, B. D., Davis, K. J., and
8 Carey, E. V.: Ecosystem respiration and its components in an old-growth forest in
9 the Great Lakes region of the United States, Agricultural and Forest Meteorology,
10 148, 171-185, 2008.

11 Vargas, R., and Allen, M. F.: Environmental controls and the influence of vegetation
12 type, fine roots and rhizomorphs on diel and seasonal variation in soil respiration,
13 New Phytologist, 179, 460-471, 10.1111/j.1469-8137.2008.02481.x, 2008a.

14 Vargas, R., and Allen, M. F.: Diel patterns of soil respiration in a tropical forest after
15 Hurricane Wilma, Journal of Geophysical Research-Biogeosciences, 113,
16 10.1029/2007jg000620, 2008b.

17 Vargas, R., and Allen, M. F.: Dynamics of fine root, fungal rhizomorphs, and soil
18 respiration in a mixed temperate forest: Integrating sensors and observations,

Vadose Zone Journal, 7, 1055-1064, 10.2136/vzj2007.0138, 2008c.

Vargas, R., Detto, M., Baldocchi, D. D., and Allen, M. F.: Multiscale analysis of temporal variability of soil CO₂ production as influenced by weather and vegetation, Global Change Biology, 16, 1589-1605, 10.1111/j.1365-2486.2009.02111.x, 2010.

Widen, B., and Lindroth, A.: A calibration system for soil carbon dioxide efflux measurement chambers: Description and application, Soil Sci. Soc. Am. J., 67, 327-334, 2003.

Xu, L. K., Baldocchi, D. D., and Tang, J. W.: How soil moisture, rain pulses, and growth alter the response of ecosystem respiration to temperature, Global Biogeochemical Cycles, 18, GB4002 4010.1029/2004GB002281, 2004.

Xu, M., and Qi, Y.: Spatial and seasonal variations of Q(10) determined by soil respiration measurements at a Sierra Nevadan forest, Global Biogeochemical Cycles, 15, 687-696, 2001.

Yuste, J. C., Janssens, I. A., Carrara, A., and Ceulemans, R.: Annual Q(10) of soil respiration reflects plant phenological patterns as well as temperature sensitivity, Global Change Biology, 10, 161-169, 2004.

Zhou, T., Shi, P. J., Hui, D. F., and Luo, Y. Q.: Global pattern of temperature sensitivity of soil heterotrophic respiration (Q(10)) and its implications for carbon-climate

1 feedback, Journal of Geophysical Research-Biogeosciences, 114, 2009.

2

Figure Legends

Fig. 1. Schematic illustration of the multi-channel automated chamber system for continuous measurement of soil CO₂ efflux. The dashed square means a water proofed aluminum casing (Field Access Case). Bold arrows indicate the direction of chamber airflow. Abbreviations: Power = DC 12 V or AC 85–240 V for the system; Charger = AC-DC convert for charging and controlling a 12 V (7.2 A·h) lead-acid battery that drives the system; Cmp = air compressor; P_{Air} = compressed air from the air tank to the pneumatic cylinders for opening and closing the chamber lids; F₂ = air filter (0.5 mm mesh); S = sample air from the chamber; P = sample pump; W_T = water trap; F₁ = air filter (1 μF mesh); IRGA = infrared gas analyzer; R = sampled air returned to the chamber.

Fig. 2. Image of the multi-channel automated chamber systems installed at the Tomakomai site (a) and a set of solid state, non-dispersive infrared gas analyzers (NDIR sensor) vertically installed at different depths of soil (b).

Fig. 3. The rate of diffusion of water vapour across the PTFE filter measured by the

humidity and temperature probes (HMP45D, Vaisala, Helsinki, Finland). Black circles represent the probe that was covered with the original filter. Gray circles indicate the probe that was enclosed with the PTFE screen.

Fig. 4. Humidity sensitivity of the solid-state CO₂ sensors (GMT222, Vaisala, Helsinki, Finland) as compared with the Li-Cor IRGA (LI-840). (a) Calibration was conducted at relative humidity of about 17% against CO₂ concentration standards. (b) Output bias at relative humidity of about 90% for the Vaisala CO₂ sensors. Symbols indicate the sensors with different serial number.

Fig. 5. The time to reach a steady-state CO₂ concentration for the LI-840 IRGA and Vaisala CO₂ probes. Three CO₂ probes were inserted into a calibration chamber with 10 L of volume; the chamber air was circulated through the LI-840 IRGA with micro-pump at flow rate of about 0.8 L min⁻¹. The chamber was firstly in a CO₂ equilibrium of 475 ppm, and then a CO₂ standard of 650 ppm was flashed through the chamber at flow rate of about 3 L min⁻¹.

Fig. 6. Seasonal changes in hourly soil temperature at 5 cm depth (a, solid line), daily

rainfall (a, bars), hourly volumetric soil moisture (a, dashed line), soil CO₂ efflux (b, solid line) and heterotrophic respiration (b, dashed line) measured by the automated chamber system, and soil CO₂ efflux measured by the soil CO₂ gradient system (c) in larch forest at Tomakomai flux site in 2003. For the chamber approach, measurements were conducted between day 108 and day 345, other values were estimated by using the Q_{10} function of Eq. (4).

Fig. 8. Effect of soil temperature at a depth of 5 cm on soil CO₂ efflux (a) and root respiration (b) at the Tomakomai site measured by the automated chamber system, and soil CO₂ efflux at the Tomakomai site measured by the soil CO₂ gradient system (c). Data points represent the hourly efflux averaged over eight chambers or two gradient plots. The solid line represents the best fitting curve of temperature-dependent Q_{10} function.

Fig. 9. Temperature normalized soil CO₂ efflux, ratio between measured soil CO₂ efflux (R_s) and its temperature fitted value ($R_s(T)$), versus volumetric soil water content. (a) and (b) represent soil CO₂ efflux and root respiration at the Tomakomai site measured by the automated chamber system, and (c) represents soil CO₂ efflux at the Tomakomai

1 site measured by the soil CO₂ gradient system.

2
3 Fig. 10. Seasonal changes in Q_{10} of soil CO₂ efflux (dots with solid line), heterotrophic
4 respiration (triangles with dashed line) and root respiration (circles with dotted line).
5 Respiration data were obtained with the automated chamber system. Root respiration
6 was estimated as soil CO₂ efflux minus heterotrophic respiration. We could not derive
7 the Q_{10} during the snow covered season even from datasets obtained with the soil CO₂
8 gradient technique, due to the fact that soil temperature was maintained very stable
9 under the snowpack (Fig. 6a).

10
11 Fig. 11. Seasonal change in the contributions of heterotrophic respiration (triangles) and
12 root respiration (circles) to the total soil CO₂ efflux. Respiration data were obtained with
13 the automated chamber system. Root respiration was estimated as soil CO₂ efflux minus
14 heterotrophic respiration.

1 **Figures**

2

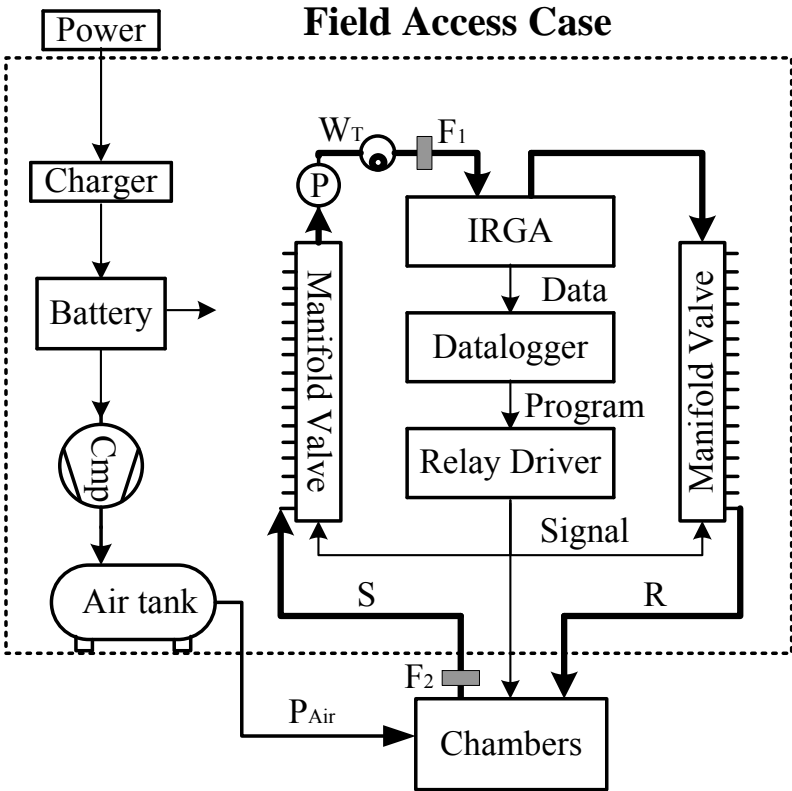


Fig. 1.

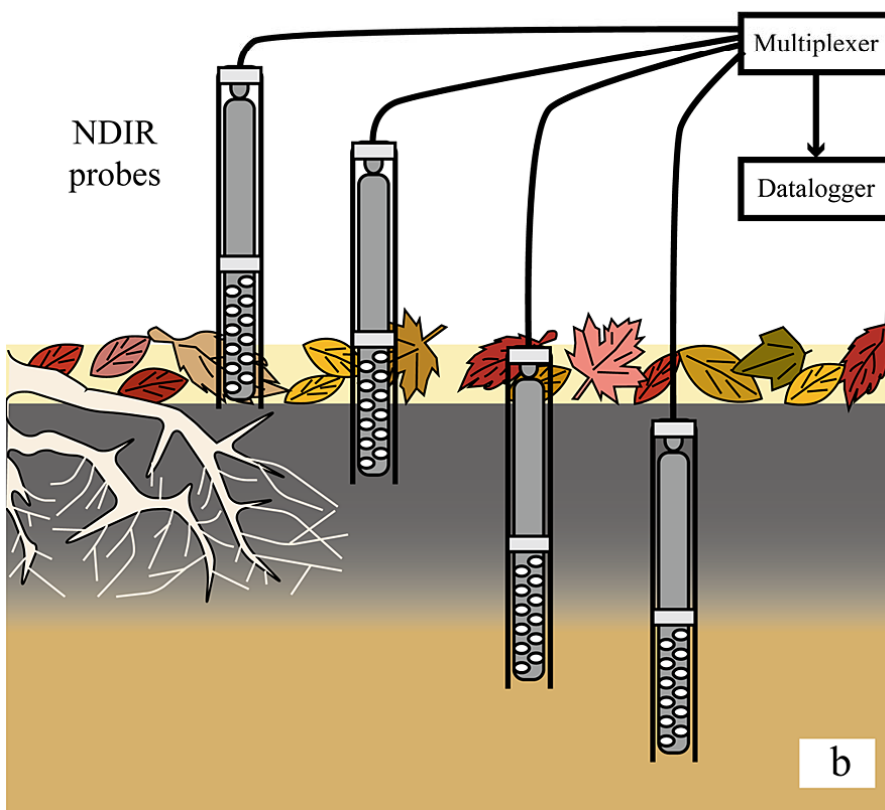


Fig. 2.

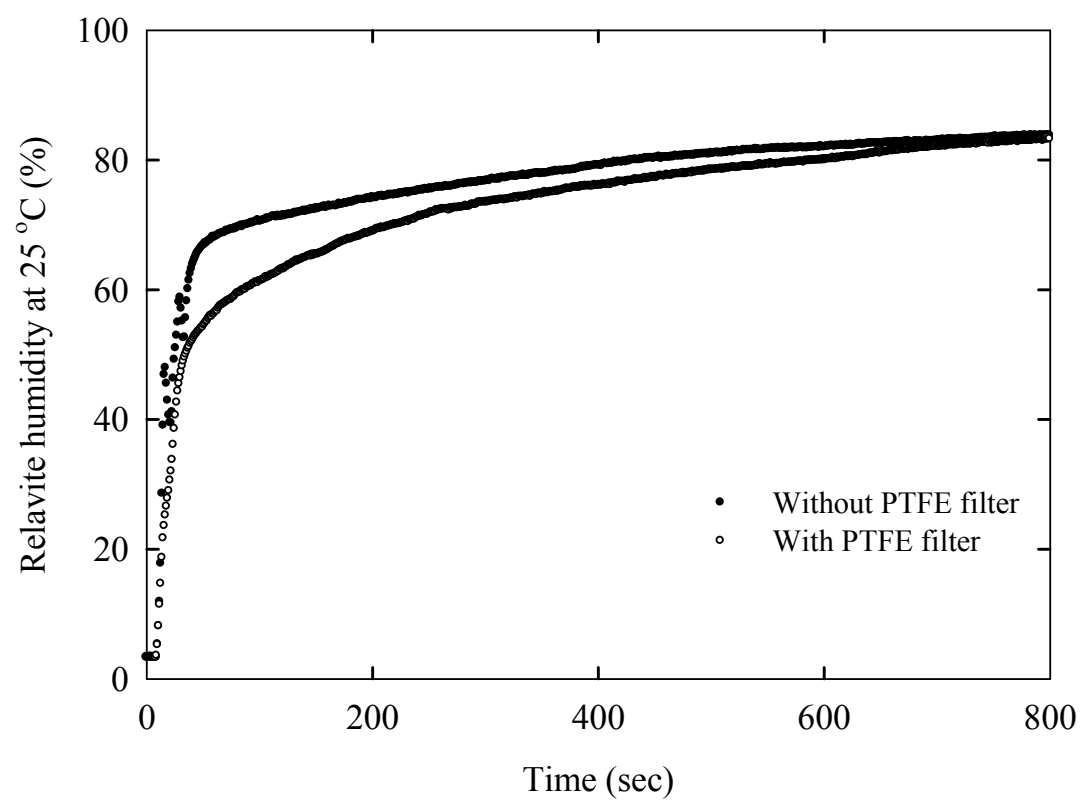


Fig. 2

1

2

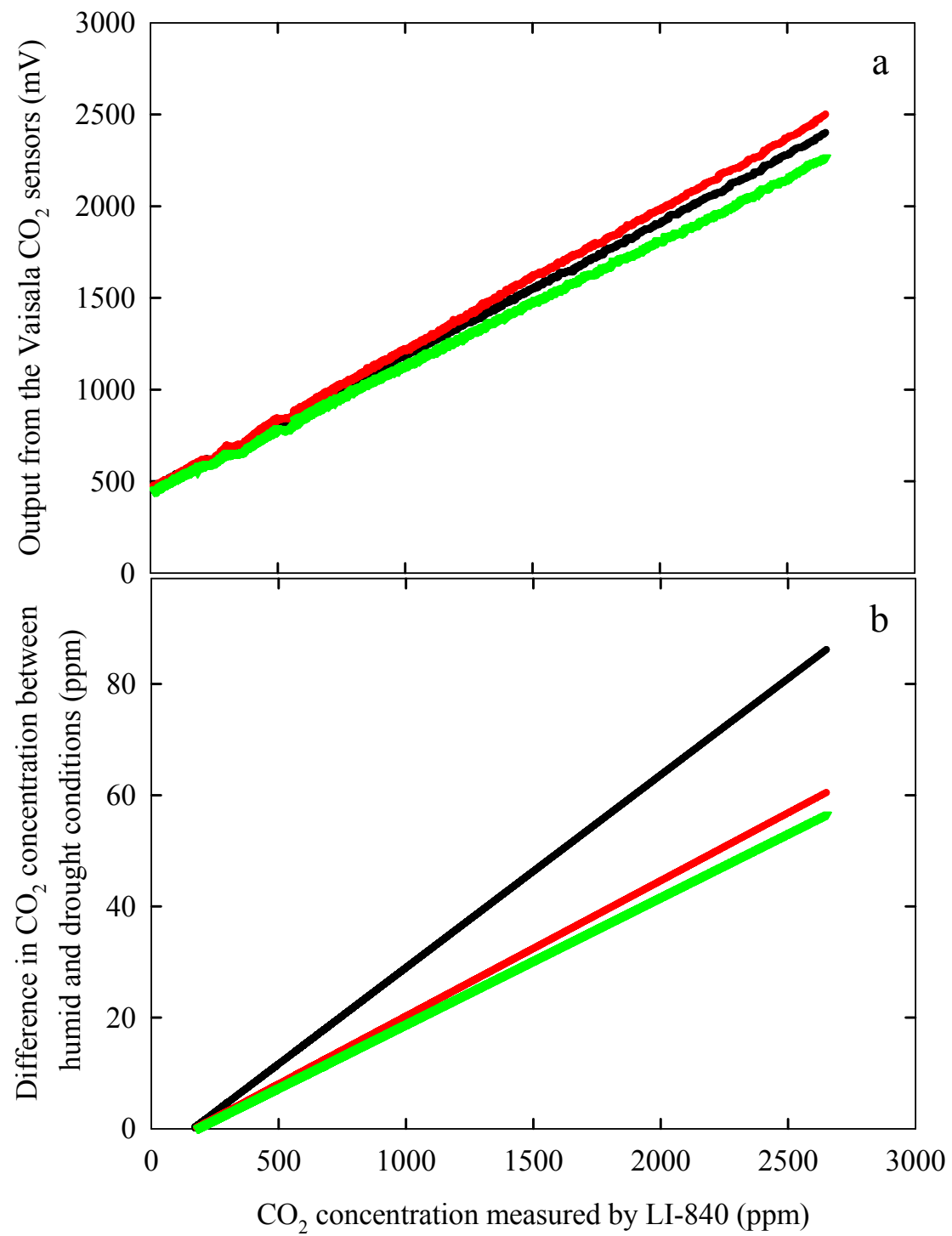


Fig. 4.

1

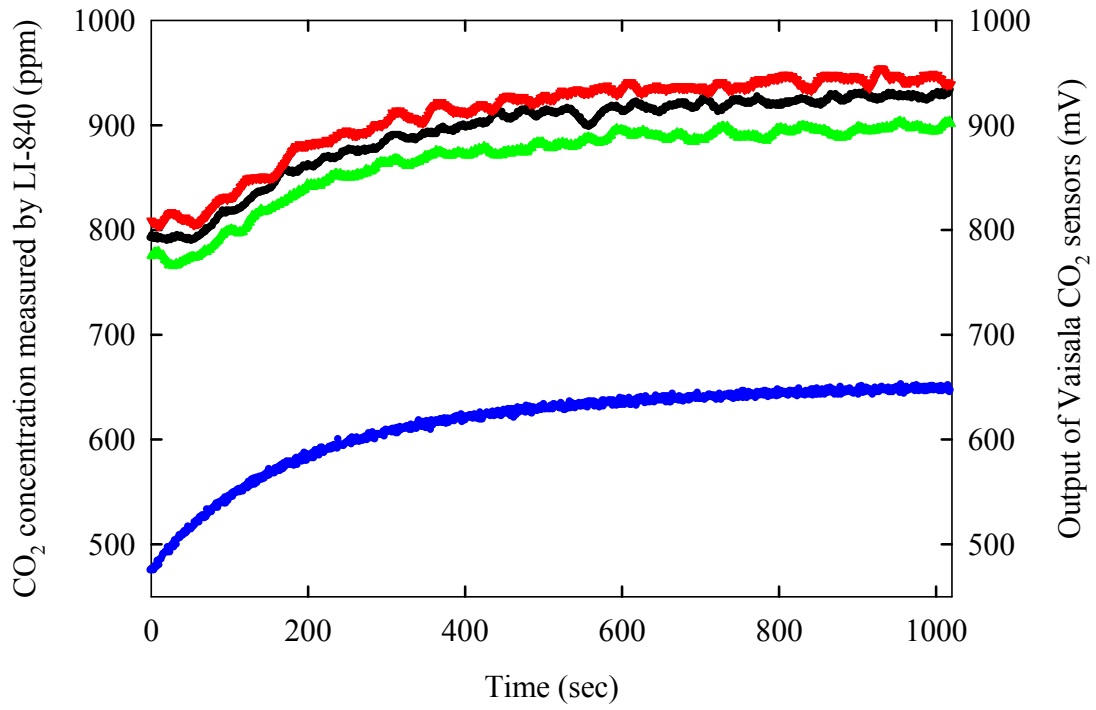


Fig. 5.

2

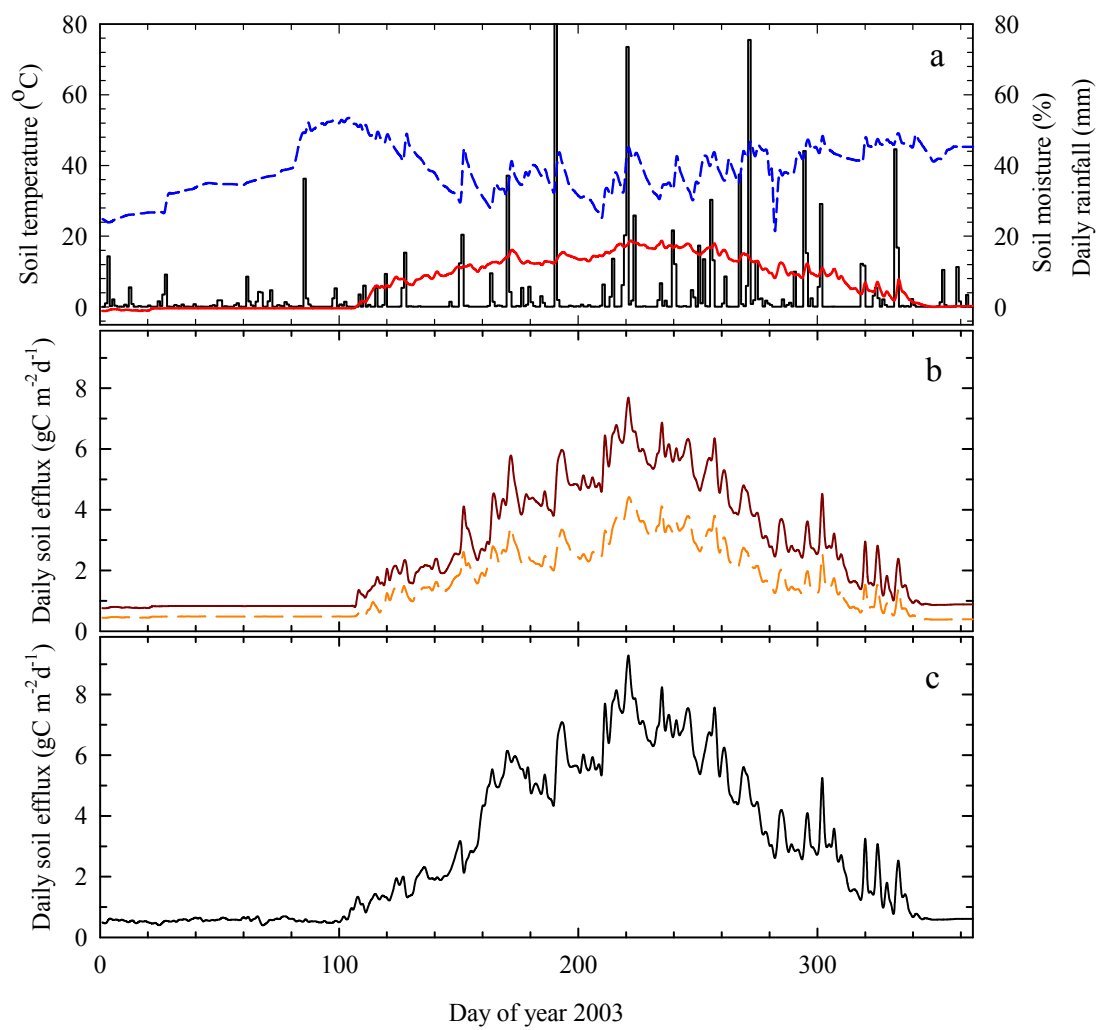


Fig. 6.

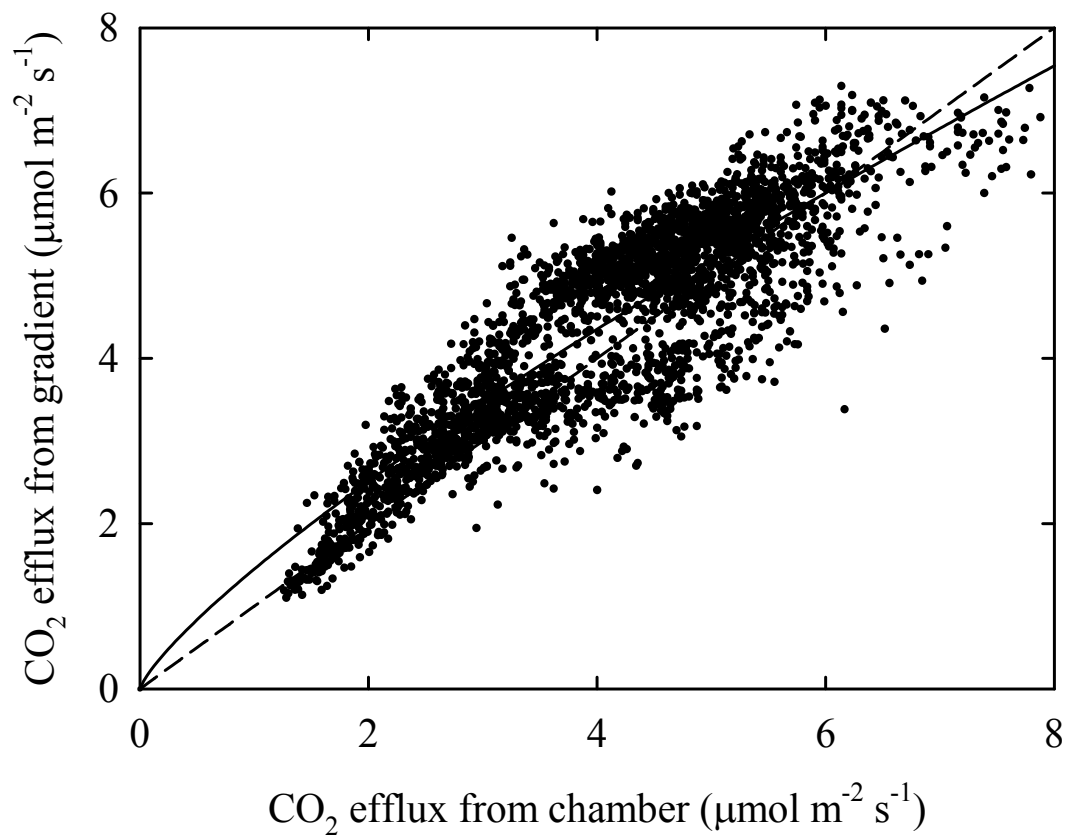


Fig. 7.

1

2

3

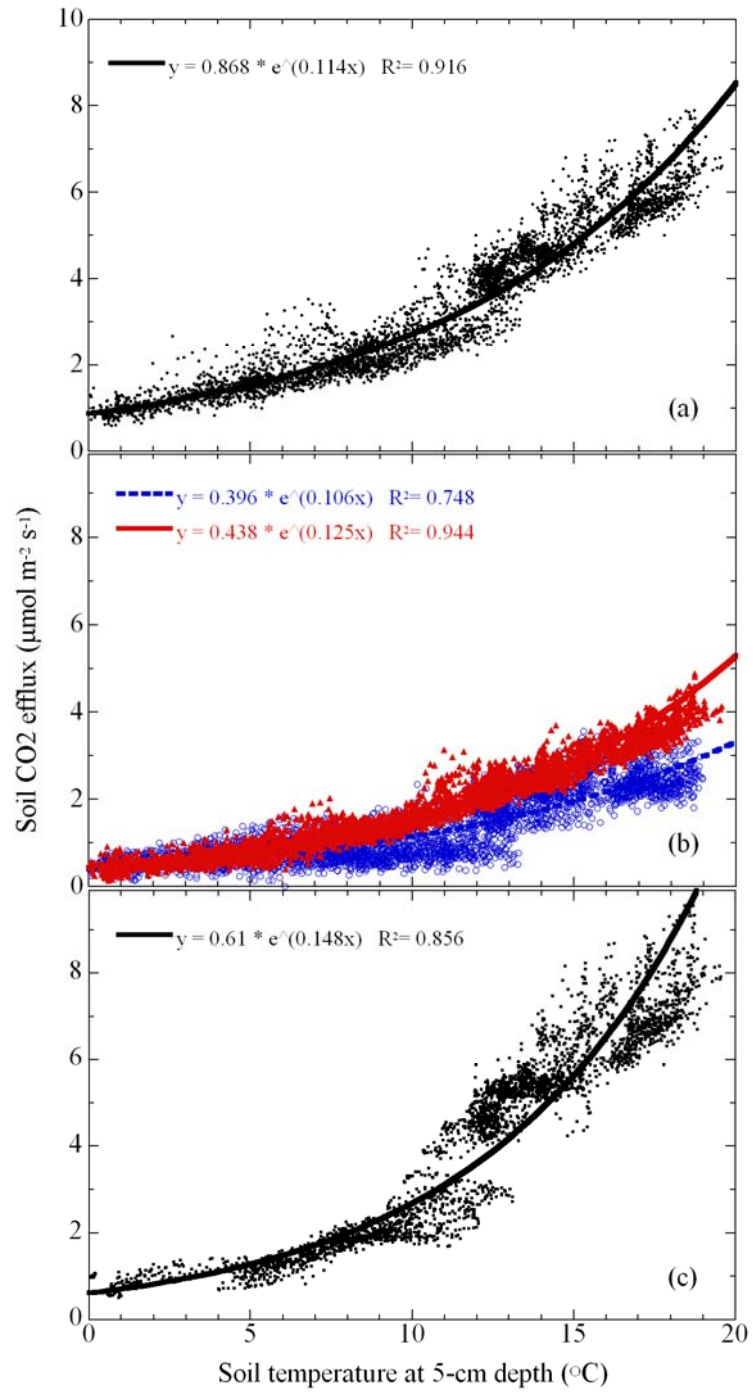
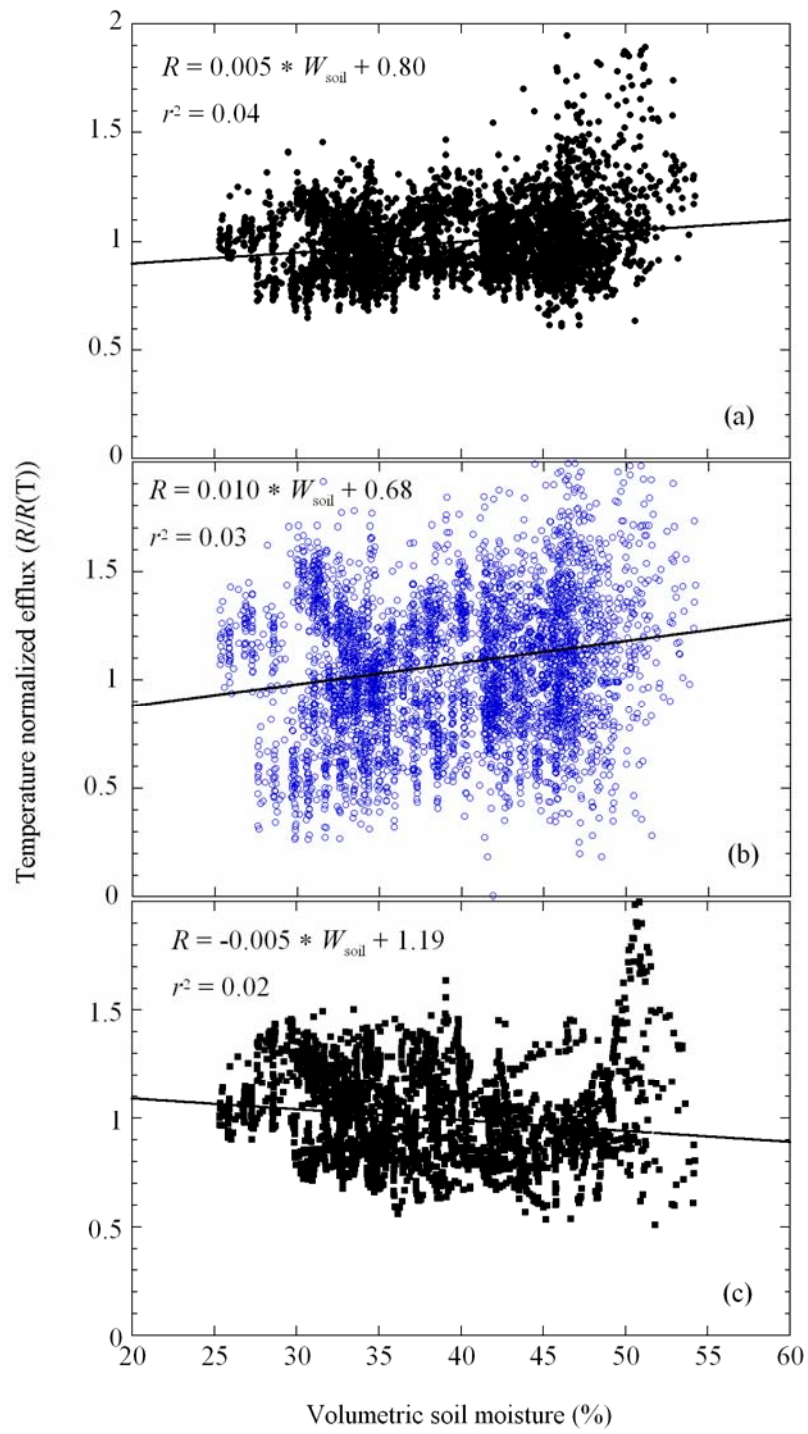


Fig. 8.



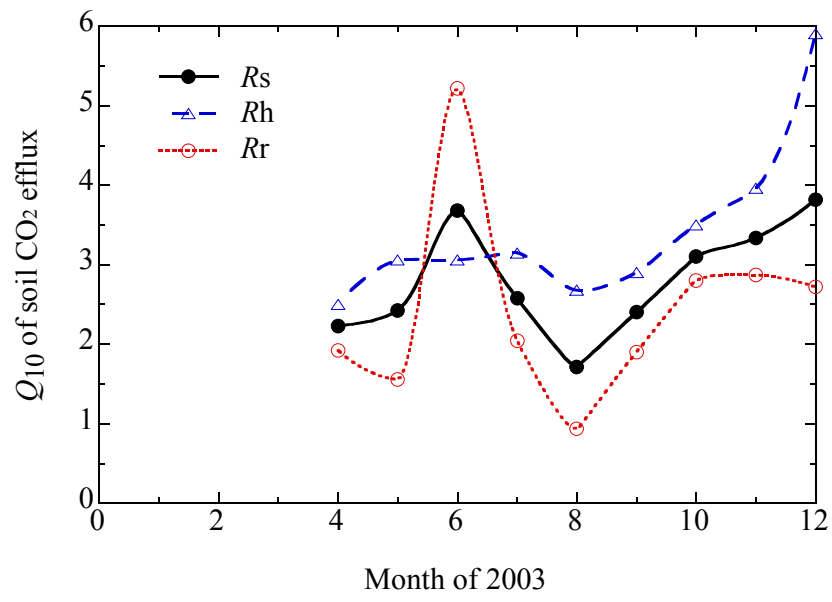


Fig. 10.

1

2

3

4

5

6

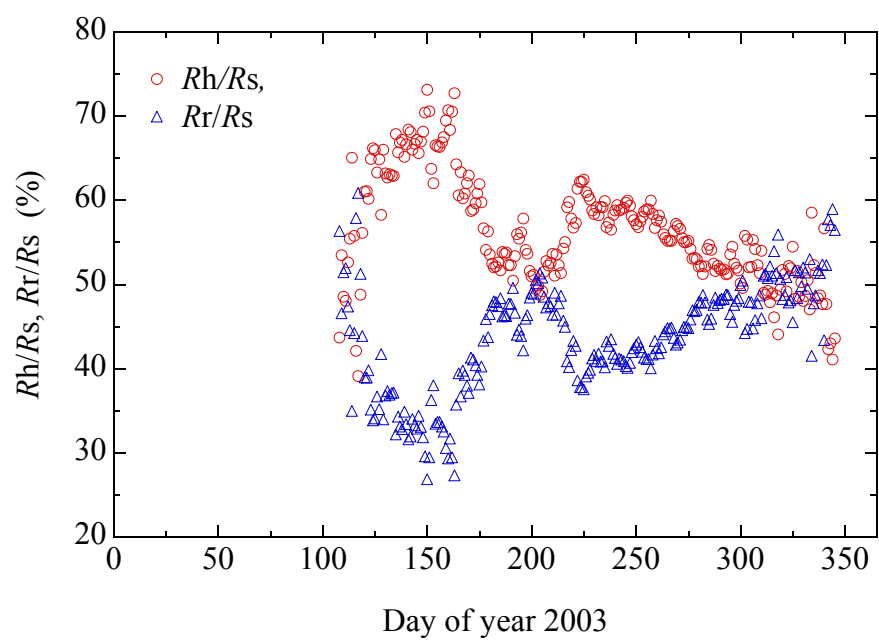


Fig. 11.

1

2